

# Chapter 3

## Coulomb Excitation

Coulomb excitation is a nuclear reaction in which a target/projectile nucleus is excited by the common electromagnetic field. Stable targets are bombarded with heavy ions at energies so low that the Coulomb repulsion prevents the particle from touching each other, thus assuring a pure Coulomb interaction process. This process has been extensively used to study the excited states in nuclei. Let us discuss the theory in detail.

### 3.1 Theoretical Description

In the collision between two heavy ions the electromagnetic interaction depends on the electromagnetic multipole moments of both nuclei, thus during the process, one or both nuclei may be excited. The excitation cross section can be expressed in terms of the same electromagnetic multipole matrix elements which also characterize the decay process. If the Coulomb excitation can be described in the semiclassical approach the calculations becomes very easy.

### 3.2 Semiclassical Theory

Although quantum-mechanical calculations are performed for heavy ion scattering, the understanding of reactions between heavy ions is greatly facilitated by applying semiclassical concepts [19, 20] to these processes. In order to decide whether a classical description is justified one should compare the wavelength  $\lambda$  (eq. 3.15) of the projectile with a dimension characteristic for the classical orbits, e.g the distance of closest approach in a head on collision  $D(\theta_{cm} = \pi)$  (eq. 3.13). If  $\lambda \ll D(\theta_{cm} = \pi)$ , one can form a wave packet which moves along a hyperbolic orbit exactly like a classical particle. It is convenient to introduce the Sommerfeld parameter which measures the strength of the Coulomb interaction i.e.,

$$\eta = \frac{D(\theta_{cm} = \pi)}{2 \cdot \lambda} = 0.157 \cdot Z_1 \cdot Z_2 \cdot \sqrt{\frac{A_1}{T_{lab}}} \quad (3.1)$$

In eq. 3.1, the numerical value is obtained for the initial energy  $T_{lab}$  expressed in MeV.  $Z_1$ ,  $A_1$  and  $Z_2$ ,  $A_2$  denote charge and mass numbers (in atomic mass unit) of projectile and target nucleus, respectively. The Sommerfeld parameter  $\eta$  is illustrated in fig. 3.1 as a function of the target charge number for various projectiles.

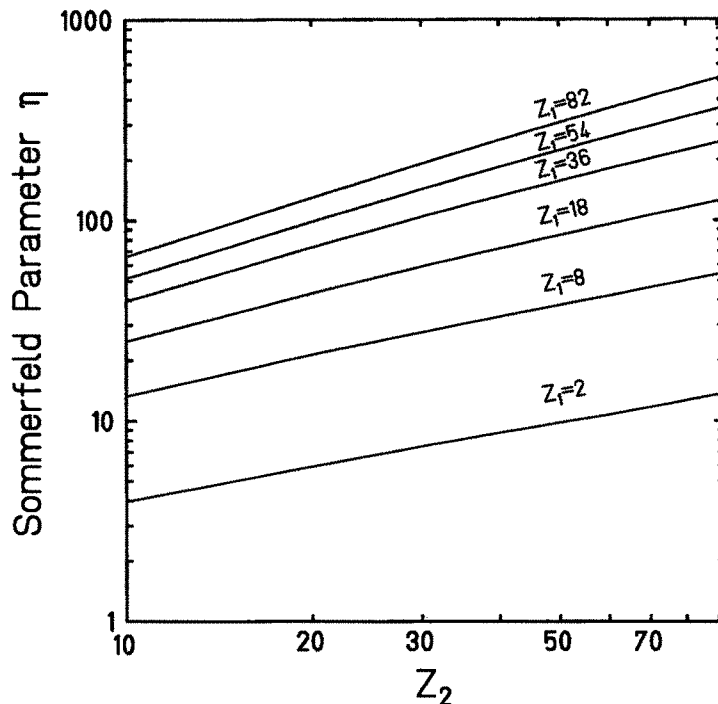


Figure 3.1: Sommerfeld parameter  $\eta$  (eq. 3.1) as a function of the target charge number  $Z_2$  for various projectiles at the safe bombarding energy (eq. 3.16).

If the Sommerfeld parameter is significantly larger than unity ( $\eta \gg 1$ ), one may describe the relative motion of the particles by classical hyperbolic orbits. In the heavy ion reaction  $^{58}\text{Ni}$  on  $^{112}\text{Sn}$  at 175 MeV investigated at IUAC the value for  $\eta = 127$  which justifies the use of semiclassical approach.

Fig. 3.2 shows the hyperbola ( $\theta_{cm}=120^\circ$ ) for the  $^{58}\text{Ni}+^{112}\text{Sn}$  system at 175 MeV, which is completely specified by the charge numbers, the energy and the scattering angle. It is usually described in its parametric representation which simultaneously determines the position of the projectile and the time in terms of a dimensionless parameter. The parameter  $\omega$  is introduced by the relations

$$r = a \cdot (\epsilon \cdot \cosh \omega + 1) \quad (3.2)$$

$$t = \frac{a}{v} \cdot (\epsilon \cdot \sinh\omega + \omega) \quad (3.3)$$

where  $\epsilon = 1/\sin(\frac{1}{2}\theta_{cm})$  is the excentricity of the classical orbit,  $v$  the projectile velocity and the quantity  $a$  is half the distance of closest approach in a head-on-collision, i.e.

$$a = \frac{0.72 \cdot Z_1 \cdot Z_2}{T_{lab}} \cdot \frac{A_1 + A_2}{A_2} \quad [fm] \quad (3.4)$$

When the parameter  $\omega$  varies from  $-\infty$  to  $+\infty$  the particle moves along the hyperbola

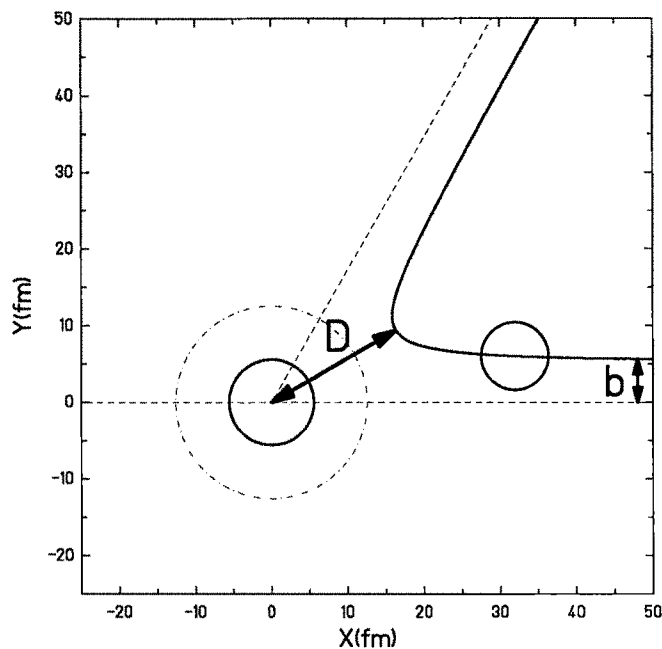


Figure 3.2: Classical picture of the  $^{58}\text{Ni}$  projectile orbit ( $\theta_{cm}=120^\circ$ ) in the Coulomb field of the  $^{112}\text{Sn}$  nucleus at 175MeV. The hyperbolic orbit of the projectile is shown in the relative frame of reference where the target is at rest. The nuclear charge radii are displayed (for details see text) as well as the nuclear interaction radius (dashed dotted lines).

in such a way that the point of closest approach is reached for  $\omega=t=0$ . In the coordinate system where the z-axis is chosen along the angular momentum  $\ell$ , the projectile coordinates are given by

$$x = a \cdot (\cosh\omega + \epsilon) \quad (3.5)$$

$$y = a \cdot \sqrt{\epsilon^2 - 1} \cdot \sinh\omega \quad (3.6)$$

$$z = 0 \quad (3.7)$$

The resulting hyperbola is symmetric around the x-axis, while the one depicted in fig. 3.2 is rotated around the z-axis with an angle of  $\vartheta_R = \frac{\theta_{cm} - \pi}{2}$ , using the following relations

$$x_1 = x \cdot \cos\vartheta_R + y \cdot \sin\vartheta_R \quad (3.8)$$

$$y_1 = -x \cdot \sin\vartheta_R + y \cdot \cos\vartheta_R \quad (3.9)$$

$$z_1 = z \quad (3.10)$$

For the hyperbola, we can determine the impact parameter  $b$  [for  $y_1(\omega = -\infty)$ ], angular momentum  $\ell$  and the distance of closest approach  $D$  [for  $r(\omega = 0)$ ] from the measured scattering angle  $\theta_{cm}$ .

$$b = a \cdot \cot \frac{\theta_{cm}}{2} \quad (3.11)$$

$$\ell = k_\infty \cdot b = \eta \cdot \cot \frac{\theta_{cm}}{2} \quad (3.12)$$

$$D = a \cdot \left[ \sin^{-1} \left( \frac{\theta_{cm}}{2} \right) + 1 \right] \quad (3.13)$$

The asymptotic wave number  $k_\infty$  is given by

$$k_\infty = 0.219 \cdot \frac{A_2}{A_1 + A_2} \cdot \sqrt{A_1 \cdot T_{lab}} \quad [fm^{-1}] \quad (3.14)$$

For the  $^{58}\text{Ni} + ^{112}\text{Sn}$  system at 175 MeV, an asymptotic wave number of  $k_\infty = 14.5 \text{ fm}^{-1}$  is calculated which yields an impact parameter of  $b = 5.05 \text{ fm}$ , an angular momentum of  $73.4 \hbar$  and a distant of closest approach of  $D = 18.8 \text{ fm}$  at a scattering angle of  $\theta_{cm} = 120^\circ$ .

The de Broglie wavelength is given by

$$\lambda = (k_\infty)^{-1} \quad (3.15)$$

We can rewrite eq. 3.13 for the special case  $\theta_{cm} = 180^\circ$  ( $D = 2a$ ) to obtain the expression for the safe bombarding energy

$$T_{safe} = \frac{1.44 \cdot Z_1 \cdot Z_2}{D} \cdot \frac{A_1 + A_2}{A_2} [MeV] \quad (3.16)$$

where  $D = C_1 + C_2 + 5.0 \text{ [fm]}$  is the safe distance.

$C_1$  and  $C_2$  are the matter half-density radii (Fermi distribution) of the collision partners [21]. For the estimates in the present section, we use

$$C_i = R_i \cdot (1 - R_i^{-2}) \quad (3.17)$$

and where  $R_i$  is the nuclear radius for a homogeneous mass distribution [22], which is parametrized as

$$R_i = 1.28 \cdot A_i^{1/3} - 0.76 + 0.8 \cdot A_i^{-1/3} \quad (3.18)$$

Isotope	$R_i$ (fm)	$C_i$ (fm)
$^{58}\text{Ni}(i=1)$	4.40	4.17
$^{112}\text{Sn}(i=2)$	5.58	5.40

Table 3.1: Nuclear charge radii for Fermi and homogeneous mass distribution

For the  $^{58}\text{Ni}+^{112}\text{Sn}$  system the nuclear charge radii are displayed in fig. 3.2 and the summarized in tab. 3.1.

Fig. 3.2 shows for completeness the nuclear interaction radius  $R_{int}=12.55\text{fm}$  which is calculated by

$$R_{int} = C_1 + C_2 + 4.49 - \frac{C_1 + C_2}{6.35} \quad [fm] \quad (3.19)$$

In the present Coulomb excitation experiment, this distance required for nuclear reactions is not reached since the incident energy of 175MeV is well below the safe bombarding energy of 210MeV for the  $^{58}\text{Ni}+^{112}\text{Sn}$  system.

### 3.3 Multipole Expansion

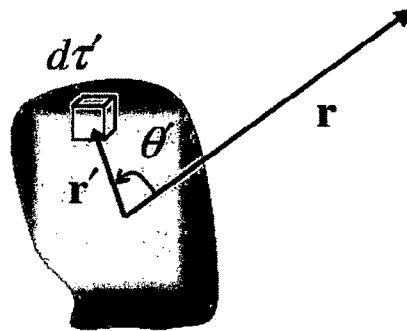


Figure 3.3: Schematic picture of an extended charge distribution (see text)

In the semiclassical approach the projectile is treated as a point object and target nucleus as an extended object (see fig. 3.3). The electric potential is defined as

$$U(\vec{r}) = \int \int \int \frac{\rho_p(\vec{r}')}{|\vec{r} - \vec{r}'|} d\tau' \quad (3.20)$$

where  $\rho_p(\vec{r}')$  is the electric charge distribution. One expands the radial dependence as a function of spherical harmonics

$$\frac{1}{|\vec{r} - \vec{r}'|} = \sum_{\ell=0}^{\infty} \frac{r'^{\ell}}{r^{\ell+1}} \cdot \frac{4\pi}{2 \cdot \ell + 1} \sum_{m=-\ell}^{\ell} Y_{\ell m}(\theta, \phi) \cdot Y_{\ell m}^*(\theta', \phi') \quad (3.21)$$

In the following we consider two physical cases:

**CASE 1: electric monopole when  $\ell=m=0$**

$$Y_{00}(\theta, \phi) = Y_{00}(\theta', \phi') = \frac{1}{\sqrt{4\pi}} \quad (3.22)$$

In this case one obtain the following radial dependence

$$\frac{1}{|\vec{r} - \vec{r}'|} = \frac{1}{r} \quad (3.23)$$

Therefore, the potential for the electric monopole is given by

$$U(\vec{r}) = \int \int \int \frac{\rho_p(\vec{r}')}{r} d\tau' \quad (3.24)$$

Inserting the homogenous charge distribution

$$\rho_p(\vec{r}') = \frac{3 \cdot Z \cdot e}{4 \cdot \pi \cdot R_0^3} \quad (3.25)$$

in eq. 3.24 one obtains, the well-known result

$$\begin{aligned} U(\vec{r}) &= \frac{3 \cdot Z \cdot e}{4 \cdot \pi \cdot R_0^3} \cdot \frac{1}{r} \cdot \int \int \int r'^2 dr' \sin\theta' d\theta' d\phi' \\ &= \frac{3 \cdot Z \cdot e}{4 \cdot \pi \cdot R_0^3} \cdot \frac{1}{r} \cdot \frac{R_0^3}{3} \cdot 4 \cdot \pi \\ &= \frac{Z \cdot e}{r} \end{aligned} \quad (3.26)$$

For point like charges, the scattering cross-section is given by the Rutherford cross section

$$\frac{d\sigma_{Ruth}}{d\Omega_{cm}} = \frac{a^2}{4} \cdot \sin^{-4} \frac{\theta_{cm}}{2} \quad (3.27)$$

**CASE 2: electric multipole when  $\ell=2, m$**

The potential is given by

$$U(\vec{r}) = \sum_{\ell=0}^{\infty} \sum_{m=-\ell}^{\ell} \frac{4 \cdot \pi}{2 \cdot \ell + 1} \cdot \frac{1}{r^{\ell+1}} \cdot Y_{\ell m}(\theta, \phi) \int \int \int \rho_p(\vec{r}') \cdot r'^{\ell} \cdot Y_{\ell m}^*(\theta', \phi') d\tau' \quad (3.28)$$

After reordering the multipole moment is defined by

$$M^*(\ell, m) = \int \int \int \rho_p(\vec{r}') \cdot r'^{\ell} \cdot Y_{\ell m}^*(\theta', \phi') d\tau' \quad (3.29)$$

The reduced transition probability  $B(E2 \uparrow)$  is related to the nuclear matrix element by the formula

$$B(E\ell = 2; I_i \rightarrow I_f) = \sum_{M_f, m} \langle I_f M_f | M(\ell = 2, m) | I_i M_i \rangle^2 \quad (3.30)$$

According to the Wigner-Eckart theorem, a matrix element of an operator  $M(\ell, m)$  leads to the following reduced matrix element

$$\langle I_f M_f | M(E2, m) | I_i M_i \rangle = (I_i 2 M_i m | I_f M_f) \langle I_f || M(E2) || I_i \rangle \quad (3.31)$$

where  $(I_i 2 M_i m | I_f M_f)$  is a Clebsch-Gordan coefficient. The reduced matrix element  $\langle I_f || M(E2) || I_i \rangle$  contains the information about the nuclear wave functions. Then, according to the orthonormality of the Clebsch-Gordan coefficients, we obtained the following expression for the  $B(E2 \uparrow)$  values:

$$B(E2; I_i \rightarrow I_f) = \frac{1}{2 \cdot I_i + 1} \langle I_f || M(E2) || I_i \rangle^2 \quad (3.32)$$

This expression assures that the lifetime of a state does not depend on its orientation (rotational invariance). Neglecting conversion coefficients, one obtains the following relation between the lifetime of a state and the reduced transition probability

$$\frac{1}{\tau} \cong 1.23 \cdot 10^{13} \cdot B(E2, I_f \rightarrow I_i) \cdot E_{\gamma}^5 \quad [s^{-1}] \quad (3.33)$$

For the scattering of point-like objects with an extended nucleus (shown in fig. 3.3), the differential inelastic cross section is given by

$$\frac{d\sigma_{i \rightarrow f}}{d\Omega_{cm}} = P_{i \rightarrow f} \cdot \frac{d\sigma_{Ruth}}{d\Omega_{cm}} \quad (3.34)$$

where  $P_{i \rightarrow f}$  is the excitation probability. For the simplest case of a one step excitation the inelastic cross section can be written analytically as

$$d\sigma_{E2} \cong 4.819 \cdot \left(1 + \frac{A_1}{A_2}\right)^{-2} \frac{A_1}{Z_2^2} \cdot T_{MeV} \cdot B(E2; I_i \rightarrow I_f) \cdot df_{E2}(\eta, \xi) [b] \quad (3.35)$$

where  $df_{E2}$  is a classical function which is closely related to the orbital integral. The function  $df_{E2}$  depends on the adiabaticity parameter  $\xi$ , which is given by

$$\xi = \frac{Z_1 \cdot Z_2 \cdot A_1^{\frac{1}{2}} \cdot \Delta E'_{MeV}}{12.65 \cdot (T_{MeV} - \frac{1}{2} \Delta E'_{MeV})^{\frac{3}{2}}} \quad (3.36)$$

where

$$\Delta E'_{MeV} = \left(1 + \frac{A_1}{A_2}\right) \cdot \Delta E_{MeV}$$

and  $\Delta E$  is the energy of an excited state. For the  $^{58}\text{Ni}+^{112}\text{Sn}$  system at 175 MeV one obtains an adiabaticity parameter of 0.70. Fig. 3.4 shows the inelastic cross section for the  $2^+$  excitation in  $^{112}\text{Sn}$ . The single step excitation was performed with a reduced transition probability of  $B(E2; 0^+ \rightarrow 2^+) = 0.240 e^2 b^2$ . One notices a maximum of the inelastic cross section which can be moved to higher scattering angles for larger adiabaticity parameter  $\xi$ . The relation of the reduced transition probability between the excitation  $B(E2 \uparrow)$  and the decay  $B(E2 \downarrow)$  of the nuclear state is given by

$$B(E2; I_f \rightarrow I_i) = \frac{2 \cdot I_i + 1}{2 \cdot I_f + 1} \cdot B(E2; I_i \rightarrow I_f) \quad (3.37)$$

since the absolute value of the reduced matrix element is invariant under the interchange of  $I_i$  and  $I_f$ . In case of an E2 transition between ground state  $0_{gs}^+$  and the first excited state  $2_1^+$ , we obtain

$$B(E2; 0_{gs}^+ \rightarrow 2_1^+) = 5 \cdot B(E2; 2_1^+ \rightarrow 0_{gs}^+) \quad (3.38)$$

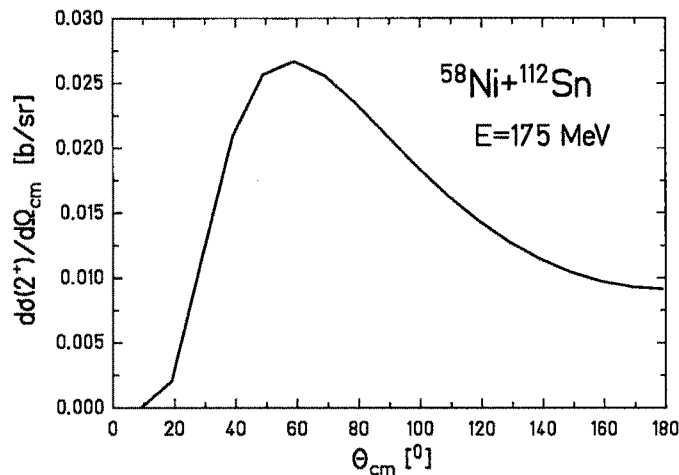


Figure 3.4: Inelastic cross section for the single-step  $2^+$  excitation in  $^{112}\text{Sn}$  ( $B(E2; 0^+ \rightarrow 2^+) = 0.240 e^2 b^2$ ) after the scattering of  $^{58}\text{Ni}$  projectiles at an energy of 175 MeV.

In the collision between two heavy ions, both target and projectile can usually be excited. In most cases one has to consider only the monopole-multipole fields, in which the monopole moments, i.e. the electric charges, are undisturbed by excitations. If the projectile is a composite particle (fig. 3.3), the process is entirely analogous to the excitation of the target nucleus, and corresponds merely to the interchange of the roles of target nucleus

and projectile. It differs from the evaluation of the target excitation through kinematical effects associated with the centre-of-mass motion ( $T_{lab}/A_1 = \text{constant}$ ). The interaction is now proportional to the projectile reduced transition probability.

In the collision of two heavy ions, where both of them may have large deformations, one has to study the effect of the multipole-multipole interactions. In most experiments these effects are, however, negligibly small.

### 3.4 Angular Distribution of De-Excitation $\gamma$ -Rays

The nuclear states populated by Coulomb excitation decay by emission of  $\gamma$ -radiation or conversion electrons. Since the time scales for the excitation process ( $10^{-22} - 10^{-21}$ s) and the  $\gamma$ -ray decay ( $10^{-15} - 10^{-9}$ s) are quite different, the differential cross section for observing both the scattered particle and the  $\gamma$ -quantum is given by the following product

$$\frac{d^2\sigma}{d\Omega_p^{lab} d\Omega_\gamma^{lab}} = \frac{d\sigma_{Ruth}}{d\Omega_{cm}} \cdot \frac{d\Omega_{cm}}{d\Omega_{lab}} \cdot \frac{dW(\gamma_{N \rightarrow M})}{d\Omega_\gamma^{rest}} \cdot \frac{d\Omega_\gamma^{rest}}{d\Omega_\gamma^{lab}} \quad (3.39)$$

where  $\frac{d\sigma_{Ruth}}{d\Omega_{cm}}$  is the Rutherford cross-section (eq. 3.27) in the centre-of-mass system. If the projectile is detected, the transformation from the cm-system to the lab-system yields

$$\frac{d\Omega_{cm}}{d\Omega_{lab}} = \frac{\sin^2\vartheta_1}{\sin^2\theta_{cm}} \cdot \cos(\theta_{cm} - \vartheta_1) \quad (3.40)$$

with

$$\theta_{cm} = \vartheta_1 + \arcsin\left(\frac{A_1}{A_2} \cdot \sin\vartheta_1\right) \quad (3.41)$$

For the detection of the target nucleus, one obtains

$$\frac{d\Omega_{cm}}{d\Omega_{lab}} = \frac{1}{4 \cdot \cos\vartheta_2} \quad (3.42)$$

The angular distribution for  $\gamma$ -quanta from an excited state N to a state M has also to be transformed from a coordinate system where the target nucleus is at rest to the laboratory coordinate system by

$$\frac{d\Omega_\gamma^{rest}}{d\Omega_\gamma^{lab}} = \left(\frac{E_\gamma}{E_{\gamma 0}}\right)^2 \quad (3.43)$$

where  $E_\gamma$  is the Doppler shifted  $\gamma$ -ray energy in the laboratory frame and  $E_{\gamma 0}$  is the transition energy between the energy levels N and M. The angular distribution may be written as

$$\frac{dW(\gamma_{N \rightarrow M})}{d\Omega_\gamma^{rest}} = (4 \cdot \pi)^{-\frac{1}{2}} \cdot \sum_{k=0,2,4} \sum_{-k \leq K \leq k} A_{kK} \cdot Q_k \cdot G_k \cdot F_{kK}(I_M, I_N) \cdot Y_{kK}(\theta_\gamma, \phi_\gamma - \phi_1) \quad (3.44)$$

where  $A_{kK}$  denote the statistical tensors of the excitation,  $Q_k$  are corrections due to the finite solid angle of the Ge-detectors [23],  $G_k$  are the deorientation coefficients [24] and

$F_k(I_M, I_N)$  are the  $\gamma\gamma$ -correlation coefficients [20]. The spherical harmonics  $Y_{kK}$  depend on the polar angles  $\theta_\gamma$  and  $\phi_\gamma$ . Fig. 3.5 shows a particle- $\gamma$  correlation with  $^{58}\text{Ni}$  projectiles being detected at angles of  $\theta_{cm} = 45^\circ$  and  $-9^\circ \leq \phi_{cm} \leq 9^\circ$  (full curve) and  $81^\circ \leq \phi_{cm} \leq 99^\circ$  (dashed curve). The  $\gamma$ -rays of the  $2^+ \rightarrow 0^+$  transition in the  $^{112}\text{Sn}$  are measured with a Ge-detector in plane ( $\phi_\gamma = 0^\circ$  or  $\phi_\gamma = 180^\circ$ ). No intergration over the finite solid angle of the Ge-detector was performed and the deorientation effect was not considered.

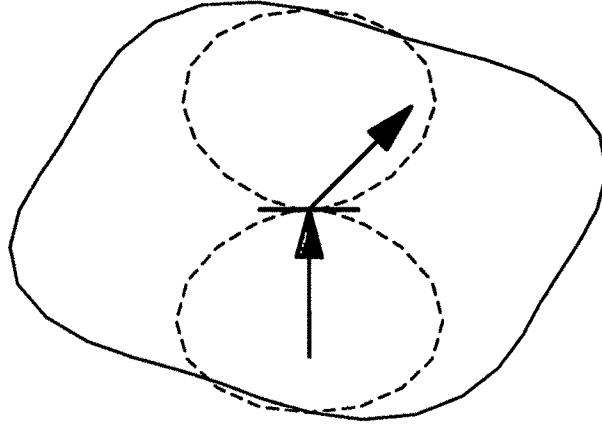


Figure 3.5: Particle- $\gamma$  angular correlation for  $^{58}\text{Ni}$  projectiles scattered at angles of  $\theta_{cm}=45^\circ$  and  $-9^\circ \leq \phi_{cm} \leq 9^\circ$  (full curve) and  $81^\circ \leq \phi_{cm} \leq 99^\circ$  (dashed curve). The  $\gamma$ -rays of the  $2^+ \rightarrow 0^+$  transition in  $^{112}\text{Sn}$  are measured with Ge-detectors in plane ( $\phi_\gamma = 0^\circ$  or  $\phi_\gamma = 180^\circ$ ). The beam and target is indicated as well as the scattering at  $\theta_{cm}=45^\circ$ .

For the geometry in which the projectiles are detected in an annular counter symmetric around the beam axis, one finds the following angular distribution:

$$\begin{aligned}
 \frac{dW(\gamma_{N \rightarrow M})}{d\Omega_{\gamma}^{rest}} &= A_{00} \cdot Q_0 \cdot G_0 \cdot F_0(0, 2) \cdot \frac{1}{2} \\
 &+ A_{20} \cdot Q_2 \cdot G_2 \cdot F_2(0, 2) \cdot \sqrt{\frac{5}{16}} \cdot (3 \cdot \cos^2 \theta_\gamma - 1) \\
 &+ A_{40} \cdot Q_4 \cdot G_4 \cdot F_4(0, 2) \\
 &\cdot \sqrt{\frac{9}{256}} \cdot (35 \cdot \cos^4 \theta_\gamma - 30 \cdot \cos^2 \theta_\gamma + 3)
 \end{aligned} \tag{3.45}$$

with the  $\gamma\gamma$ -correlation coefficients for the  $2^+ \rightarrow 0^+$  transition  $F_0(0, 2)=1$ ,  $F_2(0, 2)=-\sqrt{\frac{5}{14}}$  and  $F_4(0, 2)=-\sqrt{\frac{8}{7}}$  one obtains

$$\begin{aligned}
\frac{dW(\gamma_{N \rightarrow M})}{d\Omega_{\gamma}^{rest}} &= A_{00} \cdot Q_0 \cdot G_0 \cdot \frac{1}{2} \\
&- A_{20} \cdot Q_2 \cdot G_2 \cdot \sqrt{\frac{25}{56}} \cdot \frac{1}{2} (3 \cdot \cos^2 \theta_{\gamma} - 1) \\
&- A_{40} \cdot Q_4 \cdot G_4 \cdot \sqrt{\frac{18}{7}} \cdot \frac{1}{8} (35 \cdot \cos^4 \theta_{\gamma} - 30 \cdot \cos^2 \theta_{\gamma} + 3) \quad (3.46)
\end{aligned}$$

A  $\gamma$ -ray angular correlation for a  $2^+ \rightarrow 0^+$  transition in  $^{112}\text{Sn}$  after the scattering of  $^{58}\text{Ni}$  projectiles at an angle of  $\theta_{cm}=45^\circ$  is shown in fig. 3.6.

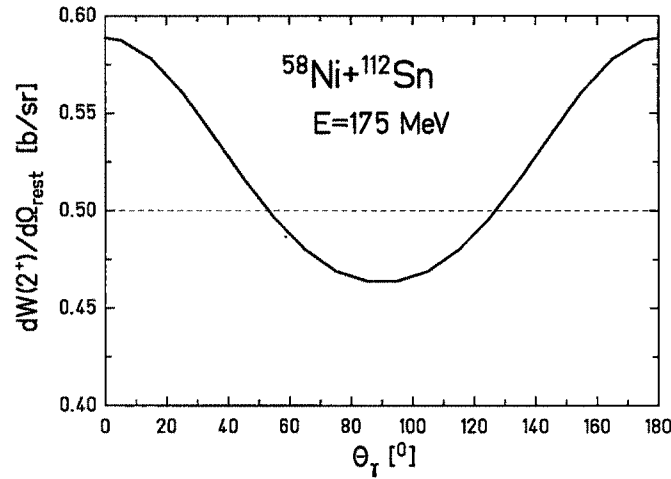


Figure 3.6:  $\gamma$ -ray angular correlation for  $2^+ \rightarrow 0^+$  transition in  $^{112}\text{Sn}$  after the scattering of  $^{58}\text{Ni}$  projectiles at an angle of  $\theta_{cm}=45^\circ$ . The calculation was performed without taking into account the deorientation effect ( $G_k=1$ ) and the integration over a finite size of the Ge detector ( $Q_k = 1$ ). The dashed line shows an isotropic  $\gamma$ -ray angular correlation.